

PACS numbers: 42.55.Lt; 42.60.Lh
DOI: 10.1070/QE2005v035n09ABEH010349

Influence of excitation parameters and active medium on the efficiency of an electric-discharge excimer ArF laser

A.M. Razhev, A.I. Shchedrin, A.G. Kalyuzhnaya, A.A. Zhupikov

Abstract. **The kinetic model of processes occurring in the plasma of an electric-discharge 193-nm excimer ArF laser operating on mixtures of He and Ne buffer gases is developed. The influence of excitation and active medium parameters on the lasing energy and total efficiency of the electric-discharge excimer ArF laser is studied theoretically and experimentally. It is shown that a specific pump power of $\sim 4.5 - 5.0$ MW cm^{-3} is required for attaining the maximum lasing energy for the highest efficiency of an ArF laser operating on a He – Ar – F_2 mixture. For the first time, the pulse energy of 1.3 J at an efficiency of 2.0 % is attained for an ArF laser with a specific pump power of 5.0 MW cm^{-3} using mixtures with helium as a buffer gas.**

Keywords: *excimer ArF laser, buffer gas, excitation parameters.*

1. Introduction

Pulsed electric-discharge 193-nm excimer ArF lasers are currently used extensively in photolithography, microelectronics, medicine and scientific research. For many of these applications, the most important parameters of the laser are the highest attainable output pulse energy at a high efficiency, a reliable and efficient laser excitation circuit, as well as its operational cost which is mainly determined by the cost of the gas mixture. It is well known that the operational cost of laser is considerably lowered if helium is used as a buffer gas instead of neon. In this context, the development of a high-power efficient laser operating on cheap gas mixtures with He as a buffer gas is a problem of topical interest. An understanding of the physical processes occurring in the gas discharge plasma is necessary for optimising the laser parameters.

The active medium pump intensity is one of the most important parameters ensuring a high output energy and a high total efficiency of the laser. For each active medium (with He or Ne as a buffer gas), there exist optimal values of the pump intensity for which the highest lasing energy is attained for the highest total efficiency of the laser. By the pump intensity we mean the specific pump power of the active medium defined as $W = E/(V\tau)$, where E is the energy stored in the peaking capacitor, V is the active volume, and τ is the duration of the first half-period of the discharge current at the base. The total efficiency of the laser in this work was defined as the ratio of the laser output energy to the energy in the storage capacitor of the excitation system.

It was shown in [1] that high values of the output energy and efficiency of a neon buffer-gas mixture ArF laser can be attained for a pump intensity of 1.8 – 2.5 MW cm^{-3}. The highest efficiency of 2.1 % for an electric-discharge ArF laser with a radiation power of 270 mJ was attained for such a pump intensity in a laser with an excitation system assembled in a capacitor-transfer type circuit and automatic UV preionisation. Depending on the experimental conditions, the active medium volume was equal to $5 \times (0.6 - 1.0) \times (2.6 - 3.2)$ cm. An output energy of 500 mJ at an efficiency of 1 % was attained in [2] for a laser similar to the one described in [1].

Similar results were also obtained in [3] using an excitation system analogous to the one considered in [1, 2]. In a Ne – He – Ar – F_2 mixture occupying a volume of 116 cm^3, a maximum efficiency of 1.3 % was attained for an output energy of 300 mJ, while the maximum output energy attained for an efficiency of 1.1 % was 420 mJ. The pump intensity was estimated at about 2.0 MW cm^{-3}. Studies of the role of buffer gases He and Ne in the laser developed in these works reveal that replacement of neon by helium lowers the output energy and efficiency by a factor of about 2.5, while lasing is quenched for charging voltages below 30 kV.

The maximum output energy was achieved in [4] for an ArF laser with a helium mixture. A circuit with a two-stage Marx generator and automatic UV preionisation were used for exciting a laser with an active volume of 500 cm^3. For a charging voltage of 70 kV and an active medium pressure of 5 atm, the output energy was 1.7 J, but the laser efficiency did not exceed 0.44 %. The total efficiency increased to 0.67 % upon a decrease in the voltage to 40 kV and pressure to 4 atm. However, the pump intensity could not be estimated in this work due to a lack of information on the voltage across the discharge gap and the duration of the discharge current.

In their theoretical studies on the effect of a buffer gas on the efficiency and output energy of ArF lasers, the authors of [5, 6] showed that the use of neon instead of

A.M. Razhev, A.A. Zhupikov Institute of Laser Physics, Siberian Branch, Russian Academy of Sciences, prosp. akad. Lavrent'eva 13/3, 630090 Novosibirsk, Russia; e-mail: razhev@laser.nsc.ru, azh@ laser.nsc.ru; web-site: www.laser.nsc.ru;
A.I. Shchedrin, A.G. Kalyuzhnaya Institute of Physics, National Academy of Sciences of Ukraine, prosp. Nauki 46, 03650 Kiev, Ukraine; e-mail: ashched@iop.kiev.ua; web-site: www.iop.kiev.ua

Received 8 June 2005
Kvantovaya Elektronika **35** (9) 799 – 804 (2005)
Translated by Ram Wadhwa

helium does not give any considerable advantage and that the effective excitation of the active medium with He as the buffer gas requires a higher pump intensity than in the case of Ne.

The results presented in [7] are slightly different from those obtained in [5] and indicate that, from the point of view of obtaining higher values of energy and efficiency, mixtures with Ne as buffer gas in an ArF laser are preferable to those with He. For the conditions considered in [7], the limiting efficiency of a gas-discharge ArF laser must be at least 4.0 %.

In our earlier work [8], we studied a $He-Ar-F_2$ mixture ArF laser in which the pump intensity was increased to 3.0 MW cm^{-3}. This made it possible to attain an output energy of 550 mJ at an efficiency of 1.3 % in an active medium of volume 130 cm^3. For the maximum efficiency of 1.5 %, the output energy was 350 mJ. A further increase in the pump intensity was hampered due to technical limitations of such an excitation system.

It follows from the literature review presented above that there is no consensus about the advantages of using helium or neon as the buffer gas. The highest lasing energy for the maximum efficiency of an ArF laser was attained in mixtures with a Ne buffer gas for an optimal pump intensity of $\sim$2.0 MW cm^{-3}. It was assumed that the replacement of Ne by He as the buffer gas would increase the pump intensity. However, its specific value ensuring the maximum output energy for the highest efficiency remains unknown.

The present paper aims at theoretical and experimental studies of the effect of excitation parameters and the active medium on the parameters of electric-discharge excimer ArF lasers operating on mixtures with He and Ne as buffer gases. Since no data are available in the literature, we shall endeavour to determine the optimal pulse intensity for which an ArF laser operating on He buffer gas mixture has simultaneously the highest efficiency and the highest output energy.

2. Experimental setup

We measured the energy and amplitude – time characteristics of voltage, current and radiation pulses in the nanosecond range. The apparatus and the measuring technique used for this purpose are described in [9].

The experimental setup used by us in the present investigations was described in detail in [10]. It should only be recalled that the excitation system consisted of an *LC* inverter circuit with a spark gap, automatic UV preionisation and a low-inductance discharge circuit. To increase the pump intensity in the excitation system used here in analogy with Ref. [10], the inductance of the basic *LC* inverter circuit was increased to 100 nH by increasing the inductance of the subcircuit between the *LC* inverter and the low-inductance discharge circuit. The effect of this inductance on the pump intensity was described in detail in [10]. Using this method for controlling the pump parameters, we were able to change the pump intensity over a wide range (up to 6.0 MW cm^{-3}).

The distance between the main electrodes in the discharge chamber of the laser was 2.7 cm. The length of the active part was 59 cm. It should be noted that the discharge width is a variable quantity that depends on the parameters of an active medium (composition and pressure) as well as pump (charging voltage). The discharge width was determined from the size of the cavern formed as a result of ablation of polymer materials. The minimum discharge width (0.7 cm) was obtained in mixtures with a helium buffer gas at the lowest pump levels, while the maximum width (1.2 cm) was obtained for the highest pump level of gas mixtures with a neon buffer gas. Thus, depending on the type of the buffer gas and the pump level, the active medium volume varied from 120 to 190 cm^3. This fact is important for a correct estimation of the pump intensity.

3. Theoretical model

We have developed in this work a theoretical model for the pump system and constructed a kinetic model of the processes occurring in the discharge plasma of a $He(Ne)-Ar-F_2$ mixture ArF laser. The results of theoretical investigations were compared with the experimental data.

In the numerical simulation of the dynamics of discharge and emission, kinetic equations were solved for the mixture components together with the equation describing the processes in the laser excitation circuit as well as the Boltzmann equation for the electron energy distribution function in an electric field [11]. The diagram of kinetic processes used for modelling the plasma kinetics in $He-Ar-F_2$ and $Ne-Ar-F_2$ gas mixtures consists of 94 reactions (Table 1). The rate of reactions (1)–(17) was calculated with the help of the Boltzmann equation. The cross sections of elastic and inelastic collisions of electrons with He and Ne atoms were borrowed from [12–14] and [13, 15–17], respectively. The cross sections of processes of interaction of electrons with argon atoms and F_2 molecules are presented in [12, 13, 17–19] and [20] respectively. The theoretical model of processes occurring in the excitation system was developed by us and described in detail in an earlier publication [10].

4. Results and discussion

In theoretical and experimental studies aimed at the attainment of the maximum lasing energy, the composition of the active gaseous medium based on the He buffer gas and its total pressure were optimised relative to the charging voltage. As a result, it was established that the theoretical composition of the gas mixture components is in good agreement with the experimentally obtained composition $He:Ar:F_2 = 79.7:20:0.3$ [8], while its optimal pressure increased from 1.7 to 2.5 atm upon an increase in the charging voltage from 20 to 32 kV. If He was replaced by Ne, the optimal pressure increased from 1.8 to 2.6 atm upon an increase in the charging voltage of the gas mixture.

In order to determine the effect of the type of buffer gas on the excitation and emission parameters of the ArF laser, we studied the discharge kinetics in the mixtures based on He and Ne. Figure 1a shows the electron energy distribution functions calculated for various electric fields in $He-Ar-F_2$ and $Ne-Ar-F_2$ gas mixtures with a constant concentration of Ar (20 %) and fluorine (0.3 %).

One can see from Fig. 1 that the presence of neon in the discharge results in a considerable increase in the fraction of electrons with energies in the interval $\sim 10-15$ eV, which can excite and ionise argon atoms (having an excitation threshold equal to 11.5 eV and an ionisation potential equal to 15.7 eV). A change in the electron energy distribution

Table 1.

Reaction No.	Reaction	Rate constant	Reference
1	$He + e \rightarrow He^* + e$	Calculated from the Boltzmann equation	
2	$He + e \rightarrow He^+ + e + e$	-"-	
3	$Ne + e \rightarrow Ne^* + e$	-"-	
4	$Ne + e \rightarrow Ne^+ + e + e$	-"-	
5	$Ne^* + e \rightarrow Ne^+ + e + e$	-"-	
6	$Ar + e \rightarrow Ar^* + e$	-"-	
7	$Ar + e \rightarrow Ar^{**} + e$	-"-	
8	$Ar + e \rightarrow Ar^+ + e + e$	-"-	
9	$Ar^* + e \rightarrow Ar^+ + e + e$	-"-	
10	$Ar^{**} + e \rightarrow Ar^+ + e + e$	-"-	
11	$Ar^* + e \rightarrow Ar^{**} + e$	-"-	
12	$Ar^{**} + e \rightarrow Ar^* + e$	-"-	
13	$F_2 + e \rightarrow F_2(\upsilon) + e$	-"-	
14	$F_2 + e \rightarrow F_2^* + e$	-"-	
15	$F_2 + e \rightarrow F_2^+ + e$	-"-	
16	$F_2 + e \rightarrow F + F^-$	-"-	
17	$F_2 + e \rightarrow F + F + e$	-"-	
18	$Ar^+ + 2He \rightarrow HeAr^+ + He$	1.0×10^{-32} cm^6 s^{-1}	[21]
19	$Ar^+ + 2Ne \rightarrow ArNe^+ + Ne$	1.0×10^{-32} cm^6 s^{-1}	[21]
20	$Ar^+ + Ar + He \rightarrow HeAr^+ + He$	8.0×10^{-32} cm^6 s^{-1}	[22]
21	$Ar^+ + Ar + He \rightarrow Ar_2^+ + He$	8.0×10^{-32} cm^6 s^{-1}	[22]
22	$Ar^+ + Ar + Ne \rightarrow Ar_2^+ + Ne$	2.5×10^{-31} ccm^6 s^{-1}	[22]
23	$Ar^+ + Ar + Ne \rightarrow ArNe^+ + Ar$	2.5×10^{-31} cm^6 s^{-1}	[22]
24	$Ar^+ + Ar + Ar \rightarrow Ar_2^+ + Ar$	3.0×10^{-31} cm^6 s^{-1}	[22]
25	$He^+ + He + He \rightarrow He_2^+ + He$	1.0×10^{-31} cm^6 s^{-1}	[21]
26	$Ne^+ + 2Ne \rightarrow Ne_2^+ + Ne$	3.0×10^{-31} cm^6 s^{-1}	[22]
27	$He^+ + He + Ar \rightarrow He_2^+ + Ar$	8.0×10^{-32} cm^6 s^{-1}	[21]
28	$He^+ + He + Ar \rightarrow HeAr^+ + He$	8.0×10^{-32} cm^6 s^{-1}	[21]
29	$He^+ + 2Ar \rightarrow HeAr^+ + Ar$	8.0×10^{-32} cm^6 s^{-1}	[21]
30	$HeAr^+ + He \rightarrow Ar^+ + 2He$	1.3×10^{-11} cm^3 s^{-1}	[21]
31	$HeAr^+ + He \rightarrow He^+ + He + Ar$	5.0×10^{-10} cm^3 s^{-1}	[23]
32	$HeAr^+ + He \rightarrow He_2^+ + Ar$	5.0×10^{-10} cm^3 s^{-1}	[23]
33	$HeAr^+ + Ar \rightarrow Ar^+ + He + Ar$	5.0×10^{-10} cm^3 s^{-1}	[23]
34	$HeAr^+ + Ar \rightarrow He^+ + 2Ar$	5.0×10^{-10} cm^3 s^{-1}	[23]
35	$HeAr^+ + Ar \rightarrow Ar_2^+ + He$	3.6×10^{-9} cm^3 s^{-1}	[21]
36	$ArNe^+ + Ar \rightarrow Ar^+ + Ar + Ne$	5.0×10^{-10} cm^3 s^{-1}	[23]
37	$ArNe^+ + Ne \rightarrow Ar^+ + 2Ne$	5.0×10^{-10} cm^3 s^{-1}	[23]
38	$ArNe^+ + Ar \rightarrow Ar_2^+ + Ne$	5.0×10^{-10} cm^3 s^{-1}	[23]
39	$He^* + He + He \rightarrow He_2^* + He$	4.3×10^{-32} cm^3 s^{-1}	[11]
40	$Ne^* + 2Ne \rightarrow Ne_2^* + Ne$	4.1×10^{-34} cm^6 s^{-1}	[24]
41	$Ar^* + Ar + Ar \rightarrow Ar_2^* + Ar$	1.0×10^{-32} cm^6 s^{-1}	[25]
42	$Ar^{**} + Ar + Ar \rightarrow Ar_2^* + Ar$	5.0×10^{-32} cm^6 s^{-1}	[26]
43	$Ar^* + Ar + He \rightarrow Ar_2^* + He$	1.0×10^{-32} cm^6 s^{-1}	[21]
44	$Ar^{**} + Ar + He \rightarrow Ar_2^* + He$	1.0×10^{-32} cm^6 s^{-1}	[21]
45	$He_2^* + e \rightarrow 2He + e$	3.8×10^{-9} cm^3 s^{-1}	[27]
46	$He^* + e \rightarrow He + e$	2.6×10^{-9} cm^3 s^{-1}	[27]
47	$He_2^* \rightarrow 2He$	3.6×10^{8} s^{-1}	[27]
48	$Ne^* + Ne^* \rightarrow Ne^+ + Ne + e$	2.5×10^{-9} cm^3 s^{-1}	[28]
49	$Ne^* + F_2 \rightarrow NeF^* + F$	5.3×10^{-10} cm^3 s^{-1}	[28]
50	$Ar^* + Ar^* \rightarrow Ar_2^+ + e$	5.0×10^{-10} cm^3 s^{-1}	[26]
51	$Ar^{**} + Ar^{**} \rightarrow Ar_2^+ + e$	5.0×10^{-10} cm^3 s^{-1}	[26]
52	$Ar^* + Ar^* \rightarrow Ar^+ + Ar + e$	5.0×10^{-10} cm^3 s^{-1}	[26]
53	$Ar^{**} + Ar^{**} \rightarrow Ar^+ + Ar + e$	5.0×10^{-10} cm^3 s^{-1}	[26]
54	$Ar_2^* + e \rightarrow 2Ar + e$	1.0×10^{-9} cm^3 s^{-1}	[30]
55	$Ar_2^* \rightarrow 2Ar$	3.12×10^{5} s^{-1}	[25]
56	$Ne_2^* \rightarrow 2Ne$	6.0×10^{4} s^{-1}	[25]
57	$Ar + He^* \rightarrow Ar^+ + He + e$	7.0×10^{-11} cm^3 s^{-1}	[31]
58	$Ne^+ + Ar \rightarrow Ar^+ + Ne$	6.0×10^{-15} cm^3 s^{-1}	[29]
59	$Ne_2^+ + Ar \rightarrow Ar^+ + 2Ne$	5.0×10^{-14} cm^3 s^{-1}	[25]
60	$F + He + e \rightarrow F^{--} + He$	6.6×10^{-34} cm^6 s^{-1}	[27]

Continuation of Table 1.

Reaction No.	Reaction	Rate constant	Reference
61	$Ar^* + F_2 \rightarrow ArF^* + F$	5.4×10^{-10} cm^3 s^{-1}	[25]
62	$Ar^{**} + F_2 \rightarrow ArF^* + F$	5.4×10^{-10} cm^3 s^{-1}	[25]
63	$Ar_2^* + F_2 \rightarrow ArF^* + Ar + F$	3.0×10^{-10} cm^3 s^{-1}	[25]
64	$He_2^+ + e \rightarrow He^* + He$	$5.0\times10^{-10}(0.026/T_e)$ cm^3 s^{-1}	[23]
65	$Ar_2^+ + e \rightarrow Ar^* + Ar$	$8.5 \times 10^{-7}(0.026/T_e)^{0.67}$ cm^3 s^{-1}	[23]
66	$Ne_2^+ + e \rightarrow Ne^* + Ne$	$1.7 \times 10^{-7}(0.026/T_e)^{0.43}$ cm^3 s^{-1}	[23]
67	$F_2^+ + F \rightarrow F_2 + F$	10^{-6} cm^3 s^{-1}	[27]
68	$Ar^+ + F^- + M \rightarrow ArF^* + M$	Calculated by using Flannery's formulas	[34]
69	$Ar_2^+ + F^- + M \rightarrow Ar_2F^* + M$	-"-	[34]
70	$He^+ + F^- + M \rightarrow He^* + F + M$	-"-	[34]
71	$He_2^+ + F^- + M \rightarrow 2He + F + M$	-"-	[34]
72	$Ne^+ + F^{--} + M \rightarrow NeF^* + M$	-"-	[34]
73	$ArF^* + Ar \rightarrow Ar + Ar + F$	9.0×10^{-12} cm^3 s^{-1}	[7]
74	$ArF^* + He \rightarrow Ar + He + F$	1.0×10^{-12} cm^3 s^{-1}	[7]
75	$ArF^* + Ne \rightarrow Ar + Ne + F$	1.6×10^{-12} cm^3 s^{-1}	[32]
76	$ArF^* + F_2 \rightarrow Ar + 3F$	1.9×10^{-9} cm^3 s^{-1}	[7]
77	$ArF^* + 2Ar \rightarrow Ar_2F^* + Ar$	5.2×10^{-31} cm^6 s^{-1}	[25]
78	$ArF^* + Ar + He \rightarrow Ar_2F^* + He$	1.0×10^{-31} cm^6 s^{-1}	[7]
79	$ArF^* + Ar + Ne \rightarrow Ar_2F^* + Ne$	3.5×10^{-31} cm^6 s^{-1}	[7]
80	$ArF^* + 2Ne \rightarrow Ar + F + 2Ne$	1.0×10^{-32} cm^6 s^{-1}	[32]
81	$ArF^* + e \rightarrow Ar + F + e$	2.0×10^{-7} cm^3 s^{-1}	[7]
82	$Ar_2F^* + He \rightarrow ArF^* + Ar + He$	1.0×10^{-12} cm^3 s^{-1}	[11]
83	$h\nu + Ne^* \rightarrow Ne^+ + e$	1.2×10^{-8} cm^3 s^{-1}	[33]
84	$h\nu + Ar^* \rightarrow Ar^+ + e$	3.0×10^{-10} cm^3 s^{-1}	[33]
85	$h\nu + Ar^{**} \rightarrow Ar^+ + e$	9.0×10^{-8} cm^3 s^{-1}	[33]
86	$h\nu + F^- \rightarrow F + e$	2.8×10^{-7} cm^3 s^{-1}	[25]
87	$h\nu + He_2^* \rightarrow He_2^+ + e$	5.7×10^{-8} cm^3 s^{-1}	[11]
88	$h\nu + Ne_2^* \rightarrow Ne_2^+ + e$	3.0×10^{-8} cm^3 s^{-1}	[7]
89	$h\nu + Ar_2^* \rightarrow Ar_2^+ + e$	3.0×10^{-8} cm^3 s^{-1}	[11]
90	$h\nu + Ar_2F^* \rightarrow ArF^* + Ar$	3.0×10^{-8} cm^3 s^{-1}	[11]
91	$h\nu + ArF^* \rightarrow ArF(X) + 2h\nu$	9.0×10^{-6} cm^3 s^{-1}	[11]
92	$h\nu + ArF(X) \rightarrow ArF^*$	9.0×10^{-6} cm^3 s^{-1}	[11]
93	$ArF^* \rightarrow ArF(X) + h\nu$	2.4×10^8 s^{-1}	[25]
94	$ArF(X) \rightarrow Ar + F$	10^9 s^{-1}	[11]

Note: (M) – buffer gas; (X) – ground state of the excimer molecule; (T_e) – electron temperature in kelvins.

function upon a replacement of He by Ne is due to the difference in the transport cross sections of electron scattering from the atoms of these gases (Fig. 1b). For low energies, the elastic scattering of electrons at Ne atoms is much weaker, and hence electrons with energies below 20 eV formed as a result of excitation and ionisation of argon atoms are accumulated in the discharge region of the mixture with neon. In He-based mixtures, such electrons are scattered effectively and move away to the low energy region. Hence, in view of the fact that the presence of neon in the working mixture increases the number of electrons capable of effectively exciting and ionising the atoms of the working noble gas, the breakdown of discharge gap in such a medium occurs slightly earlier than in the medium with He as a buffer gas.

Figure 2 shows the time dependences of the discharge breakdown voltage in $He(Ne):Ar:F_2 = 79.7:20:0.3$ mixtures, calculated under a pressure of 1.9 atm and a charging voltage of 22 kV. The breakdown voltage in buffer gas mixtures with He and Ne is 36 and 31 kV, respectively. The time interval between the onset of UV preionisation and the instant of the discharge breakdown decreases from 140 to 120 ns, which may adversely affect the homogeneity of the volume discharge [35, 36].

Moreover, it was observed that a replacement of He by Ne also decreases the time of energy depostion into the discharge. In other words, the duration of the first half-period of the discharge current decreases from 40 to 35 ns, other conditions remaining the same. Hence, a replacement of He by Ne in the ArF laser mixture leads to a decrease in the energy contribution. The results of calculations were confirmed in the experiments and match with the results obtained in [5, 6].

The dependence of the voltage U across the discharge gap and current J through it on the charging voltage U_1 for the $He-Ar-F_2$ mixture was obtained both theoretically and experimentally (Fig. 3). One can see from Fig. 3 that an increase in the charging voltage from 20 to 32 kV increases the voltage across the discharge gap from 35 to 50 kV and the current from 76 to 100 kA. The optimal pressure of the gas mixture increased from 1.7 to 2.5 atm upon an increase in the charging voltage.

The nature of these dependences does not change upon a replacement of He by Ne, but the voltage across the

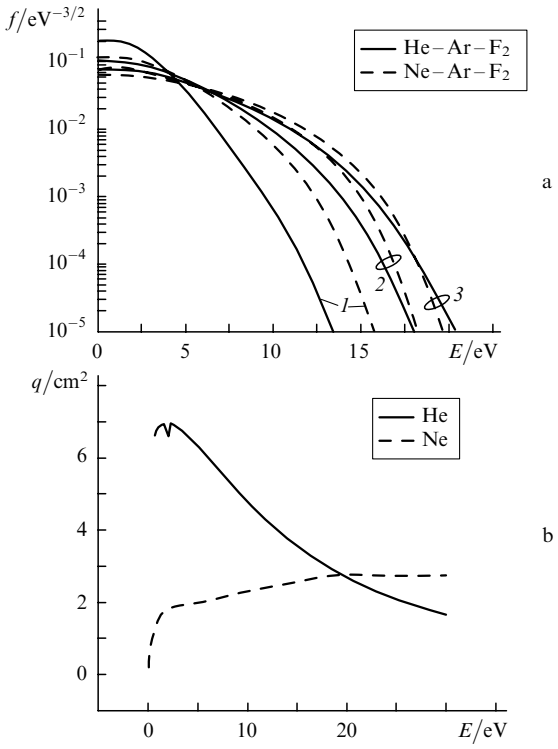

Figure 1. (a) Electron energy distribution function in He(Ne) : Ar : F_2 = 79.7 : 20 : 0.3 mixtures under a pressure $p = 2.5$ atm in the electric field of 4 (*1*), 8 (*2*) and 12 kV cm^{-1} (*3*); (b) transport cross sections q of electron scattering by helium and neon atoms.

discharge gap is lower and changes from 32 to 44 kV, while the optimal pressure of the gas mixture remains practically the same and increases from 1.8 to 2.6 atm upon an increase in the charging voltage. However, the discharge current remains virtually the same in both cases, which is in accord with the theoretical results. It was mentioned above that an increase in the charging voltage also increases the discharge gap width from 0.7 to 1.1 cm in He mixtures and from 0.8 to 1.2 cm in Ne mixtures. We took into account this circumstance during the theoretical analysis and found that the active volume increases upon an increase in the energy deposited into the active medium. Using such an appro-ach, we obtained a good agreement between the theoretical results and the results of experimental investigations.

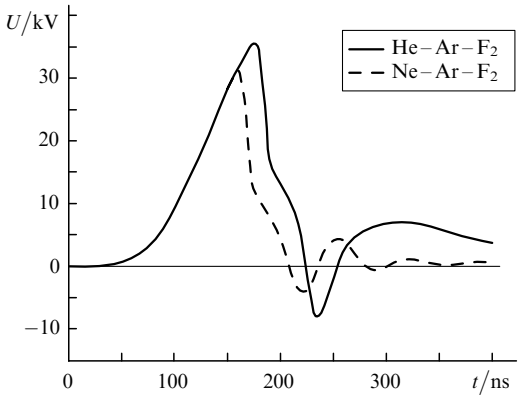

Figure 2. Time dependence of the voltage U across the discharge gap in He(Ne) : Ar : F_2 = 79.7 : 20 : 0.3 mixtures under a pressure $p = 1.9$ atm and a charging voltage of 22 kV.

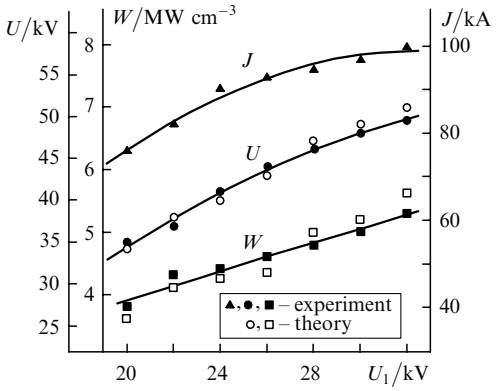

Figure 3. Theoretical and experimental dependences of the voltage U across the discharge gap, discharge current J and pump intensity W on the charging voltage U_1 for the He–Ar–F_2 mixture.

In analogy with [1, 10], we estimated the pump intensity for the He–Ar–F_2 mixture. It was found that an increase in the charging voltage U_1 from 20 to 32 kV and in the active medium volume of the laser from 120 to 180 cm^3 for a constant duration (at the base) of the first half-period of the discharge current $\tau \approx 40$ ns increases the pump intensity W from 3.8 to 5.3 MW cm^{-3} (Fig. 3). It was found in such estimates for Ne-based mixtures that upon an increase in the laser active medium volume from 145 to 190 cm^3 and for $\tau = 35$ ns, the pump intensity W increases from 3.0 to 4.4 MW cm^{-3}.

It was shown that record-high values of the lasing energy and efficiency of a ArF laser with a He buffer-gas-based active medium are obtained upon an increase in the total pressure and the active medium volume with the charging voltage, and upon the attainment of a high pump intensity W. Figure 4 shows the dependence of the laser output energy E_{out} and the total efficiency η of an ArF laser on the charging voltage U_1 for He(Ne) : Ar : F_2 = 79.7 : 20 : 0.3 mixtures. One can see that an increase in the charging voltage increases the output energy of a He mixture laser from 0.4 to 1.35 J, while the efficiency attains its highest value. Thus, a lasing energy of 1.3 J at an efficiency of 2.0 % was obtained in an ArF laser operating on He : Ar : F_2 = 79.7 : 20 : 0.3 mixtures having a volume of 175 cm^3 under a pressure of 2.4 atm and a pump intensity of 5.0 MW cm^{-3}.

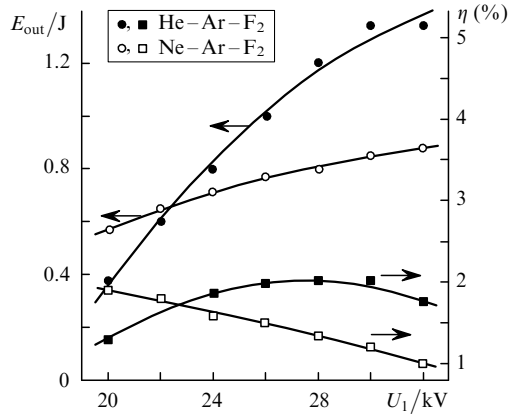

Figure 4. Experimental dependences of the output energy E_{out} and the total efficiency η of an ArF laser on the charging voltage U_1 for the active media He–Ar–F_2 and Ne–Ar–F_2.

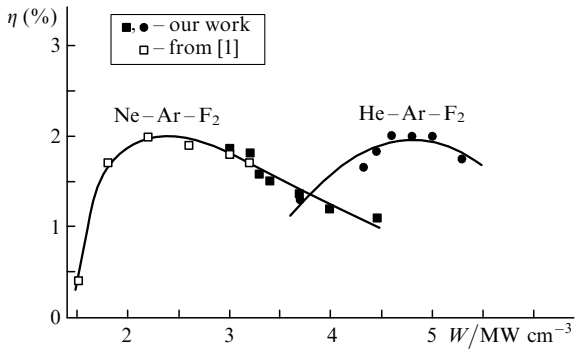

Figure 5. Dependence of the total efficiency η of an ArF laser on the pump intensity W for the active media $He-Ar-F_2$ and $Ne-Ar-F_2$.

An increase in the charging voltage leads to a slower increase in the output energy (from 0.5 to 0.88 J) in the active medium of an ArF laser with Ne buffer gas than in the case of He based mixtures. The highest efficiency is attained for a minimum charging voltage and decreases monotonically from 1.9 % to 1.1 %.

The results obtained for an ArF laser with Ne as a buffer gas (Fig. 4) can be interpreted from the point of view of attainment of the optimal pump intensity. Figure 5 shows the dependence of the total efficiency η of an ArF laser for active media based on He or Ne buffer gas on the pump intensity W. It follows from the results presented in [1] that the optimal pump intensity is 1.8–2.5 MW cm^{-3} for the $Ne-Ar-F_2$ mixture (see Fig. 5). In the present research, we used pump intensities exceeding 3.0 MW cm^{-3}; in other words, we extended the $\eta(W)$ dependence to the region of higher pump intensities and obtained a good agreement with the results obtained in [1]. The results of theoretical investigations reveal that the decrease in the total efficiency for a pump intensity higher than the optimal value is associated with a decrease in the output energy due to a stronger quenching of ArF^* molecules by the discharge electrons.

The results of our investigations showed the range of optimal pump intensities in a $He-Ar-F_2$-mixture ArF laser for which the highest value of total efficiency was obtained. It can be seen from Fig. 5 that for such excitation conditions, the optimal range of pump intensities is 4.5–5.0 MW cm^{-3}. It should be remarked that the total efficiency is almost identical for both active media with He and Ne, but is attained for different pump intensities – 2.0 and 5.0 MW cm^{-3}, respectively.

5. Conclusions

We have performed theoretical and experimental studies of the effect of excitation and active medium parameters on the output energy and efficiency of an electric-discharge 193-nm excimer ArF laser operating on $He(Ne)-Ar-F_2$ mixtures. It is shown that the highest output energy can be achieved at the maximum efficiency for an optimal intensity of the active medium pump. For a $He-Ar-F_2$ mixture ArF laser, the optimal pump intensity is 4.5–5.0 MW cm^{-3}, which is much higher than for the analogous $Ne-Ar-F_2$ mixture ArF laser. For the first time, a lasing energy of 1.3 J at an efficiency of 2.0 % was obtained in an ArF laser operating on mixtures with composition $He:Ar:F_2 = 79.7:20:0.3$ with an active volume of 175 cm^3 under a pressure of 2.4 atm and a pump intensity of 5.0 MW cm^{-3}.

References

1. Borisov V.M., Bragin I.E., Vinokhodov A.Yu., Vodchits V.A. *Kvantovaya Elektron.*, **22**, 533 (1995) [*Quantum Electron.*, **25**, 507 (1995)].
2. Borisov V.M., Borisov A.V., Bragin I.E. *Kvantovaya Elektron.*, **22**, 446 (1995) [*Quantum Electron.*, **25**, 421 (1995)].
3. Miyazaki K., Hasama T., Yamada K., et al. *J. Appl. Phys.*, **60** (8), 2721 (1986).
4. Andrew I., Dyer P., Roebuck P. *Opt. Commun.*, **49**, 189 (1984).
5. Ohwa M., Obara M. *J. Appl. Phys*, **63** (5), 1306 (1988).
6. Nagai S., Furuhashi H., Uchida Y., et al. *J. Appl. Phys.*, **77** (7), 2906 (1995).
7. Boichenko A.M., Derzhiev V.I., Zhidkov A.G., Yakovlenko S.I. *Kvantovaya Elektron.*, **19**, 486 (1992) [*Quantum Electron.*, **22**, 444 (1992)].
8. Razhev A.M., Zhupikov A.A. *Kvantovaya Elektron.*, **24**, 683 (1997) [*Quantum Electron.*, **27**, 665 (1997)].
9. Razhev A.M., Zhupikov A.A., Kargapol'tsev E.S. *Kvantovaya Elektron.*, **34**, 95 (2004) [*Quantum Electron.*, **34**, 95 (2004)].
10. Razhev A.M., Schedrin A.I., Kalyuzhnaya A.G., Zhupikov A.A. *Kvantovaya Elektron.*, **34**, 901 (2004) [*Quantum Electron.*, **34**, 901 (2004)].
11. Lo D., Shchedrin A.I., Ryabtsev A.V. *J. Phys. D*, **29**, 43 (1996).
12. http://www.kinema.com/sigmalib.dat.
13. Rejoub R., Lindsay B.G., Stebbings R.F. *Phys. Rev. A*, **65**, 042713 (2002).
14. Saha H.P. *Phys. Rev. A*, **40**, 2977 (1989).
15. Saha H.P. *Phys. Rev. A*, **39**, 5048 (1989).
16. Tachibana K., Phelps A.V. *Phys. Rev. A*, **36**, 999 (1987).
17. Hyman H.A. *Phys. Rev. A*, **20**, 855 (1979).
18. Dasgupta A., Blaha M., Giuliani J.L. *Phys. Rev. A*, **61**, 012703 (2000).
19. Hyman H.A. *Phys. Rev. A*, **18**, 441 (1978).
20. Hayashi M., Nimura T. *J. Appl. Phys.*, **54**, 4879 (1983).
21. Babichev D.N., Karelin A.V., Simakhova O.V. *Kvantovaya Elektron.*, **31**, 209 (2001) [*Quantum Electron*, **31**, 209 (2001)].
22. Dickinson A.S., Roberts R.E., Bernstein R.B. *J. Phys. B*, **5**, 355 (1972).
23. Ivanov V.A. *Usp. Fiz. Nauk*, **162**, 35 (1992).
24. Hokazono H., Midorikawa K., Obara M., et al. *J. Appl. Phys.*, **56**, 680 (1982).
25. Rhodes C.K. (Ed.) *Excimer Lasers* (New York: Springer-Verlag, 1979; Moscow: Mir, 1981).
26. Lam S.K., Zheng C.E., Lo D., Dem'yanov A., Napartovich A.P. *J. Phys. D*, **33**, 242 (2000).
27. Arteev M.S., Bunkin F.V., Derzhiev V.I., et al. *Kvantovaya Elektron.*, **13**, 2191 (1986) [*Sov. J. Quantum Electron.*, **16**, 1448 (1986)].
28. Richeboeuf L., Pasquiers S., Legentil M., Puech V. *J. Phys. D*, **31**, 373 (1998).
29. Anicich V.G. *J. Phys. Chem. Ref. Data*, **22**, 1469 (1993).
30. Takahashi A., Okada T. *Jap. J. Appl. Phys*, **37** (4A), L390 (1998).
31. Bourene M., Dutuit O., Le Calve J. *J. Chem. Phys.*, **63**, 1668 (1975).
32. Mandl A. *J. Appl. Phys.*, **53**, 1435 (1986).
33. Duzy C., Hyman H.A. *Phys. Rev. A*, **22**, 1878 (1980).
34. Flannery M.R., Yang T.P. *Appl. Phys. Lett.*, **32**, 327 (1978).
35. Hsia J. *Appl. Phys. Lett.*, **30**, 101 (1977).
36. Luches A., Nassisi V., Perrone M.R. *J. Phys. E*, **20**, 1015 (1987).